Original Article

JOURNAL OF REINFORCED PLASTICS & COMPOSITES

Journal of Reinforced Plastics and Composites
0(0) 1–12

DOI: 10.1177/0731684416684020
journals.sagepub.com/home/jrp
SAGE

Hybrid effect of carbon nanotube film and ultrathin carbon fiber prepreg composites

Jiao Pan[1], Min Li[1], Shaokai Wang[1], Yizhuo Gu[1], Qingwen Li[2] and Zuoguang Zhang[1]

Abstract

This paper successfully interlaced floating catalyst chemical vapor deposition-grown carbon nanotube film and ultrathin carbon fiber prepreg to achieve strong and flexible carbon nanotube/carbon fiber hybrid composites with high carbon nanotube loading. Epoxidation was also introduced to improve interlaminar interfacial bonding. It was found that pristine carbon nanotube film/carbon fiber interply hybrid composite (carbon fiber/carbon nanotube/carbon fiber) showed sudden and brittle failure, while epoxidation caused a gradual failure behavior. Hybrid effect analysis suggested that the improved tensile performance and synergistic effect of epoxidized carbon nanotube film/carbon fiber hybrid composite were attributed to good load transfer and suppressed delamination induced by improved interfacial bonding. In addition carbon fiber/carbon nanotube/carbon fiber manifested excellent damping capacity with the maximum loss factor of 0.13. The in-plane electrical conductivity of composite with global carbon nanotube content of 21 wt% increased to the same order of magnitude as carbon nanotube film composite. The excellent mechanical, damping, and electrical properties demonstrated great potential for both structural and multifunctional applications of the resultant hybrid composites.

Keywords

Carbon nanotube, carbon fiber, hybrid effect, interface modification, damping properties, electrical properties

Introduction

Carbon nanotubes (CNTs) possess excellent mechanical and physical properties.[1–6] These extraordinary properties endow CNT-reinforced composites multifunctionalities for the applications of structural damping,[7,8] electrostatic discharge (ESD),[9,10] electromagnetic interference (EMI) shielding,[11,12] structural health monitoring (SHM),[13,14] and lightning strike protection.[15] However, the reinforcing effect of CNTs is still far below expectation, even less than that of carbon fibers (CFs).[16] Combining CNTs with CFs for a synergistic effect presents a shortcut to take full use of structural and multifunctional advantages of these two components.

Many efforts have been devoted to fabricate CNT/CF multiscale hybrid composites via dispersing CNT in polymer matrix,[17] depositing CNTs on carbon fabric by electrophoresis,[18] introducing vertically aligned CNTs (VACNTs) by direct growth,[19] transfer printing,[20] bonding,[21] and stacking[22] techniques. Thostenson and coworkers[18,23,24] found that the hierarchical composite structure with CNT coating on CFs from electrophoretic deposition process exhibited significant increases in interlaminar shear strength, fracture resistance, and electrical conductivity. The integration of multiwalled carbon nanotubes (MWCNTs) did not compromise in-plane mechanical performance. Garcia et al.[20] prepared

[1]Key Laboratory of Aerospace Advanced Materials and Performance (Ministry of Education), School of Materials Science and Engineering, Beihang University, Beijing, China
[2]Suzhou Institute of Nano-Tech and Nano-Bionics, Suzhou, China

Corresponding author:
Shaokai Wang, Key Laboratory of Aerospace Advanced Materials and Performance (Ministry of Education), School of Materials Science and Engineering, Beihang University, No. 37 Xueyuan Road, Haidian District, Beijing 100191, China.
Email: wsk@buaa.edu.cn

interlaminar nanostitched architecture by introducing VACNTs at the interface between CF plies using a transfer-printing scheme and also observed significant increases in fracture toughness. Zeng et al.[22] designed and fabricated VACNT-based sandwich composites by stacking VACNTs and CF fabrics and then infiltrating with epoxy resin. This sandwich composite exhibited high flexural rigidity and damping, due to the effective integration of VACNTs as an interfacial layer between CF stacks. Boroujeni et al.[25] fabricated hybrid CNT–CF composites and demonstrated 11 and 35% improvements of tensile strength and ductility, respectively. Khan et al.[26] prepared carbon fiber-reinforced polymer composites (CFRPs) containing MWCNTs and found the increases of dynamic loss modulus. Although these methods successfully achieved multiscale hybrid composites, it still remains a challenge to design and prepare high CNT loading composite with more feasible manufacturing process.

Commercial available large-scale free-standing floating catalyst chemical vapor deposition (FCCVD)-grown CNT films[27,28] offer new avenues for designing high-performance interply hybrid composites. Xu et al.[29] found that FCCVD-grown CNT film interleaved CF composites showed great enhancement of flexural strength, interlaminar shear strength, and electrical conductivity. In order to design reasonable hybrid structure with synergistic effect, interfacial bonding[30–32] and hybrid effect[33,34] are two urgent issues. In our previous study,[33] we prepared aerospace quality CNT film/CF hybrid composites, and the electrical conductivity was effectively enhanced while the tensile strength moderately decreased and delamination was observed. This suggested that improvement of interfacial bonding of CNT layer was essential in future studies. In addition, many researches[35–37] have been done to investigate the hybrid effect of different fiber reinforcements. However, little research has been done to investigate the hybrid effect of CNT film and CF. Integrating thin CF prepreg with CNT film could easily achieve hybrid composite in a large range of hybrid ratio due to their similar thickness. Also, applying thin CF plies in composites has been reported to generate superior mechanical properties due to the onset shift of damage toward higher strains,[38,39] which was also expected to occur in the hybrid composite.

In this study, FCCVD-grown CNT film and ultrathin CF prepreg were used to fabricate CNT film/CF interply hybrid composite with high CNT loading. The influences of integration of CNT film and its epoxidation on hybrid effect of tensile properties, dynamic mechanical properties, and electrical conductivity of the resultant hybrid composites were investigated.

Materials and methods

Materials

Randomly oriented CNT film was synthesized using a FCCVD-growth method. In the FCCVD process, the mixture of ethanol (carbon source), ferrocene (catalyst-containing compound), and thiophene (sulfur-containing promoter) was injected into a heated gas flow reactor at a feeding rate of $0.15\,ml\,min^{-1}$. Ar–H_2 gas mixture (volume ratio 1: 1) was flowed through the reactor tube at a rate of $4000\,ml\,min^{-1}$, and the heating reaction region was about 1300°C. The detailed fabrication process has been reported in our previous researches.[5,40,41] These CNT films were about 12 μm thick, with an areal density of approximately $4.8\,g\,m^{-2}$. The CNTs fabricated by this method have 3–8 walls and an average diameter of 6–10 nm.

A unidirectional T300/epoxy prepreg with a thickness of about 30 μm was chosen to facilitate the fabrication of high CNT loading hybrid composite. The prepreg was supplied by Weihai Tuozhan Fiber Co., Ltd. which had an areal density of $40\,g\,m^{-2}$ and a resin content of 50 wt%.

In order to introduce epoxy rings on MWCNTs and improve interfacial bonding,[42–44] *m*-chloroperbenzoic acid (*m*-CPBA) with 75 wt% purity was purchased from Shanghai Aladdin Bio-Chem Technology Co., Ltd. Dichloromethane (CH_2Cl_2) and ethanol in chemical purity were purchased from Beijing Chemical Works.

Fabrication of CNT film/CF interply hybrid composites

Figure 1 shows the manufacturing process of CNT film/CF interply hybrid composites. Structure design and manufacturing parameter determined its final process quality of the hybrid composite. Both pristine and epoxidized CNT film were used to prepare hybrid composite. Epoxidized CNT films may improve the interfacial bonding between CNTs and epoxy resin matrix. Figure 1(a) shows the functionalization process. Pristine CNT films were first placed in *m*-CPBA/CH_2Cl_2 solution with concentration of 1 wt% and then washed with dichloromethane and ethanol to remove residual *m*-CPBA. Subsequently, the epoxidized CNT films were dried to remove the solvent and ready for composite fabrication.

The high resin content of the ultrathin CF prepreg was beneficial to the full impregnation of dry CNT film. During the process, resin in CF ply was partly absorbed by CNT film along through-thickness direction. CNT film showed high resin absorptive capacity due to high capillary pressure.[33] In a previous report,[41]

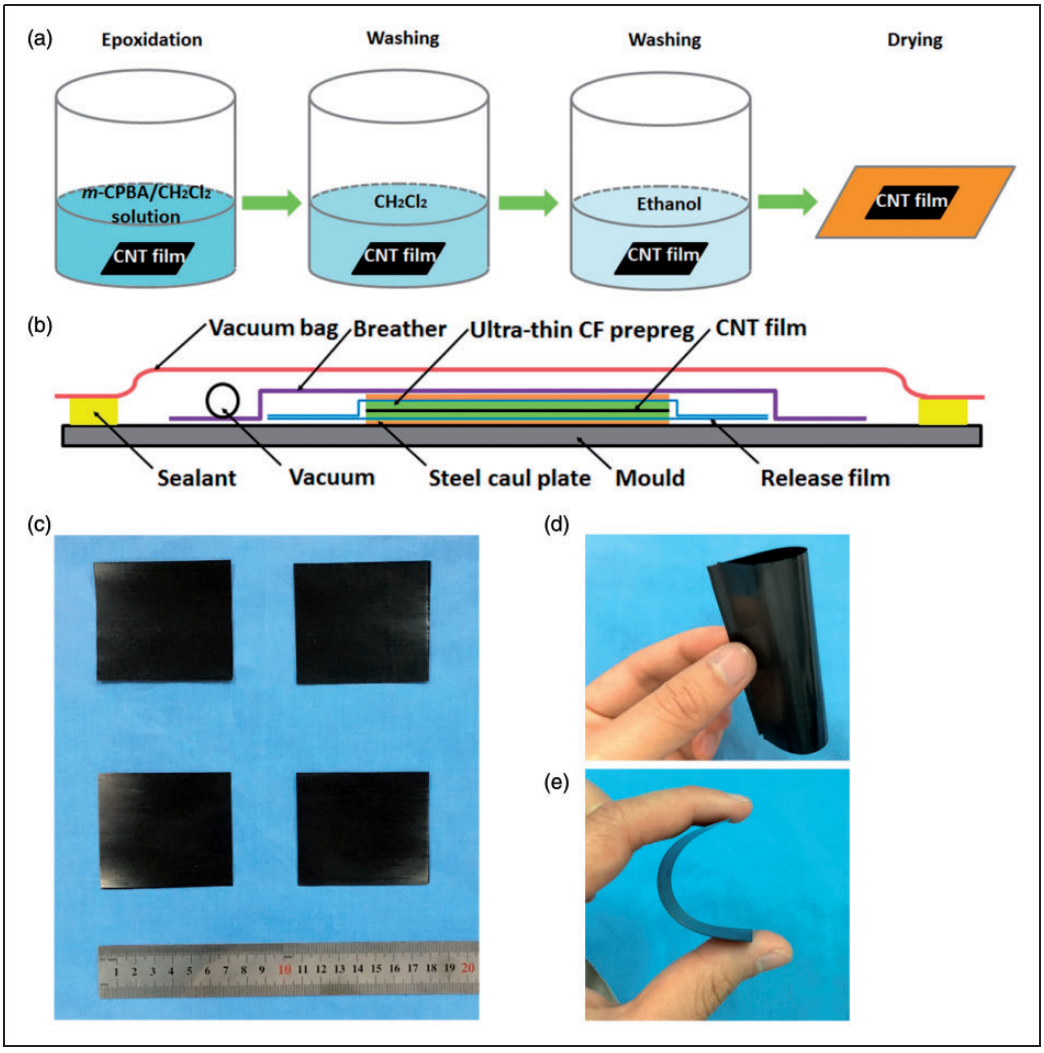

Figure 1. Manufacturing process of CNT film/CF interply hybrid composites: (a) epoxidation process of CNT film, (b) zero-bleeding autoclave process, (c) finished CNT film/CF interply hybrid composite samples, (d) super flexibility of thin-ply hybrid composite in transverse, and (e) fiber axial directions.
CF: carbon fiber; CNT: carbon nanotube.

we demonstrated that CNT film/epoxy composites show optimal tensile performance with the epoxy content of 55 wt%. In order to avoid excessive resin flow from CF ply to CNT ply, it is critical to control the resin content in CF prepregs. Thus, a bleeding process was adopted to extrude excessive resin in CF prepreg before hybridization, insuring that final fiber volume fraction in CF ply was around 60 vol% and resin content was about 55 wt% in CNT ply. The layup stacked by CF prepregs and dry CNT film was cured via a zero-bleeding autoclave process at 80°C and 0.6 MPa for 1 h to promote resin flow, which was followed by a curing process at 130°C and 0.6 MPa for 2 h. The overall layup sequence from bottom to top on the mold surface was in the following order as in Figure 1(b): steel caul plate, release film, interply hybrid structure made of CF prepreg and CNT film, breather, and vacuum bagging film. The steel caul plates were used to prevent fold defects on the surfaces.

CNT film/CF interply hybrid composites with different CNT loadings and stacking sequences were fabricated, including [CNT/CF/CNT], [CF/CNT], [CF/CNT/CF], and [CF/E-CNT/CF]. Herein, pristine and epoxidized CNT films were denoted as CNT and E-CNT, respectively. Moreover, control samples reinforced by CF, pristine, and epoxidized CNT film alone were also prepared (denoted as [CF/CF/CF], [CNT], and [E-CNT]). As shown in Figure 1(c), these finished CNT film/CF interply hybrid composite samples had excellent surface quality. In addition, these samples possessed super flexibility both in transverse and fiber axial direction, as shown in Figure 1(d) and (e).

Characterization methods

The weight of CF prepreg, CNT film, and final composite was measured by an electronic balance (Mettler Toledo ME104) with a sensibility of 0.1 mg. The structure and quality of the composites were observed using an optical microscope (OPM, Leica DM4000M). Based on these morphologies, the average thicknesses of individual ply and final composite were measured.

The wettability between epoxy and CNT film was characterized by sessile drop method using OCA20 (Data Physics Instruments GmbH, Filderstadt, Germany). A epoxy droplet of 5 µl fell onto the film and then the film was placed in an oven at 80°C for 1 h to allow the resin to fully impregnate the film. The contour was then captured to calculate the quasi-static contact angle. Three specimens were tested for each sample.

For the measurement of tensile properties, these composites were cut into $50 \times 2\,mm^2$ rectangular strips. The width and thickness were measured by OPM and micrometer caliper, respectively. The sample gauge length was 20 mm. The tensile test was conducted at a crosshead speed of $0.5\,mm\,min^{-1}$, and Instron 3344 with a load cell of 2 kN was used. Five specimens were tested for each tensile property. The tensile fractures of the composites were coated with gold and observed by scanning electron microscope (JOEL JSM-6010).

The dynamic mechanical properties of composites were tested in a tensile mode with a frequency of 1 Hz by Mettler Toledo T101423E TTDMA. Rectangular specimens with the dimension of 30 mm (length) × 5 mm (width) were prepared for dynamic mechanical analysis (DMA) tests. The gauge length was 15 mm. The static force was set as 0.05 N and the displacement was 20 µm. Temperature ramping was conducted from RT to 250°C at a heating rate of $5°C\,min^{-1}$. The glass transition temperature (Tg) was denoted as the peak temperature in the energy dissipation or tanδ curve.

In-plane electrical conductivity was measured via a two-point method by an auto DC low ohm meter (Changzhou Tonghui Electronic Co., Ltd TH2512). The two ends of the sample were polished and electrodes were connected using silver paste for better contact. Three specimens were tested for each electrical test.

Results and discussion

Structural characteristics of CNT film/CF interply hybrid composites

Figure 2 shows the typical cross-sectional morphologies of the CF control sample and the interply hybrid composites. Fibers were evenly distributed in CF control sample. The interply hybrid structure was clearly observed in Figure 2(b) and (c). CNT layer was laminated between adjacent CF layers without observable resin-rich areas or void defects. Notably, the thickness of CNT layer in [CF/E-CNT/CF] (15 µm) was larger than that of [CF/CNT/CF] (12 µm). This suggested that epoxidized CNT film showed stronger swelling effect during resin impregnation.[45,46] This phenomenon was closely related to the enhanced absorbing ability of epoxidized CNT film, which was further evidenced by the quasi-static contact angle result, as shown in Figure 3. The contact angles were $27.3 \pm 2.0°$ and $21.4 \pm 0.7°$ for pristine and epoxidized CNT film, respectively. This indicated that resin had a better wettability with epoxidized CNT film, and consequently, more resin was absorbed.

Table 1 lists the structural parameters of CNT film/CF interply hybrid composites and the corresponding control samples. Structural parameters of hybrid composites were controlled at a suitable condition, in which local fiber volume fractions in CF plies were approximately 60 vol% and local CNT contents in

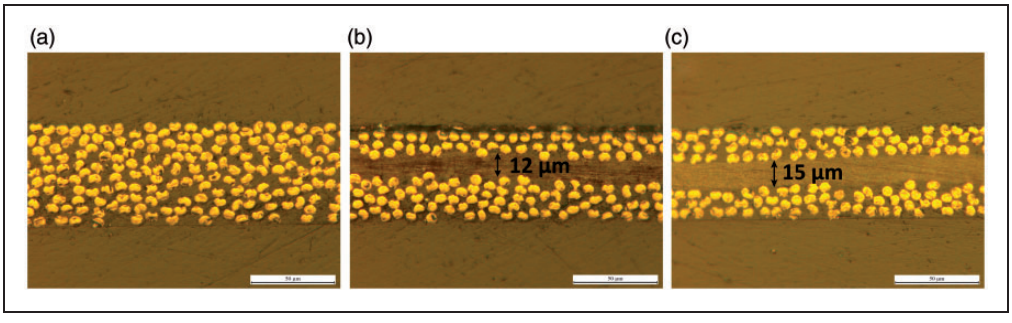

Figure 2. Cross-section morphologies of composites: (a) [CF/CF/CF], (b) [CF/CNT/CF], and (c) [CF/E-CNT/CF]. CF: carbon fiber; CNT: carbon nanotube.

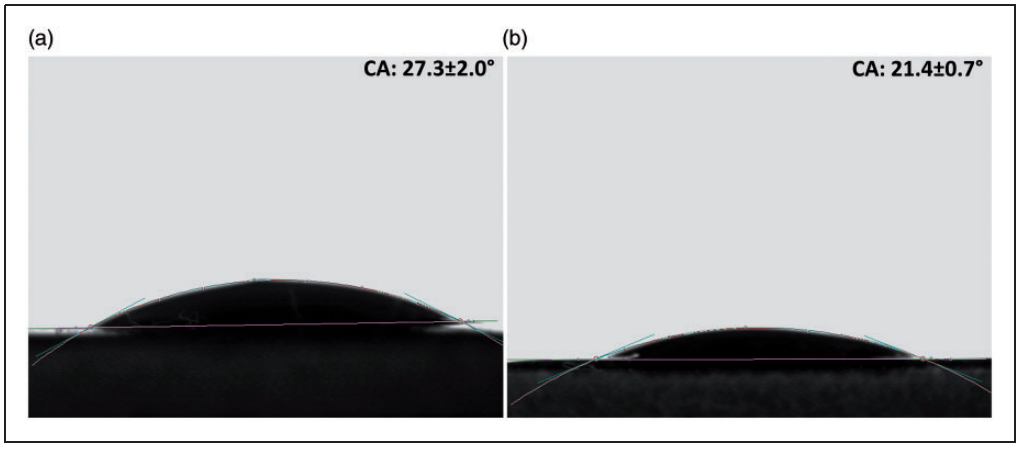

Figure 3. Images of quasi-static contact angle between (a) pristine CNT film/epoxy and (b) epoxidized CNT film/epoxy at 80°C. CNT: carbon nanotube.

Table 1. Structural parameters of CNT film/CF interply hybrid composites and the corresponding control samples.

Layup	Thickness (μm)		Local fiber volume fraction (vol%)	Local CNT content (wt%)	Global content (wt%)		
	Composite	CNT ply	CF ply	CNT ply	Fiber	CNT	Resin
[CF/CF/CF]	58	–	57.5	–	69.6	–	30.4
[CNT]	12	12	–	56.7	–	56.7	43.3
[E-CNT]	11	11	–	51.9	–	51.9	48.1
[CNT/CF/CNT]	46	26	55.6	53.3	39.5	21.1	39.4
[CF/CNT]	30	11	58.5	44.8	49.9	11.2	38.9
[CF/CNT/CF]	53	12	55.4	53.9	57.1	6.7	36.2
[CF/E-CNT/CF]	53	15	57.5	47.7	56.7	6.9	36.4

CF: carbon fiber; CNT: carbon nanotube.

CNT plies were at around 50 wt%, close to our expectations. Even though [CF/CNT/CF] and [CF/E-CNT/CF] had the same thickness, resin distribution showed difference. Local CNT content in CNT ply of [CF/E-CNT/CF] was lower than that of [CF/CNT/CF], which was consistent with the cross-sectional morphology.

Hybrid effects on tensile properties of CNT film/CF composites

Figure 4 shows the tensile properties of CNT film/CF interply hybrid composites and the corresponding control composites. As shown in Figure 4(a), [CF/CNT/CF] showed sudden and brittle failure. For [CF/E-CNT/CF], as strain increased, the tensile curve deviated from linearity (pointed out by red arrow in Figure 4(a)), and a gradual failure was observed. Figure 4(b) compared the tensile strength, modulus, and breaking elongation for the samples with different ply scheme. The hybrid composite [CF/CNT/CF] had an average tensile strength of 1609 MPa and a modulus of 61 GPa. The modified hybrid composite [CF/E-CNT/CF] showed a higher tensile strength of 1789 MPa and a modulus of 76 GPa. The tensile properties of both samples were comparable to the unidirectional T300 CFRPs for high-performance structural applications. Compared to [CF/CNT/CF], the tensile strength and modulus of [CF/E-CNT/CF] were enhanced by 11 and 25%, respectively.

According to the rule of mixture, Young's modulus E of interply hybrid composites can be described as equation (1) [47]

$$\begin{aligned} E &= E_{CF} \bullet V_{CF} + E_{CNT} \bullet (1 - V_{CF}) \\ &= (E_{CF} - E_{CNT}) \bullet V_{CF} + E_{CNT} \end{aligned} \quad (1)$$

where E_{CF} and E_{CNT} are Young's moduli of CF and CNT layer, respectively. V_{CF} is defined as the volume fraction of CF ply, and it can be calculated from the ratio of CF ply thickness to composite thickness.

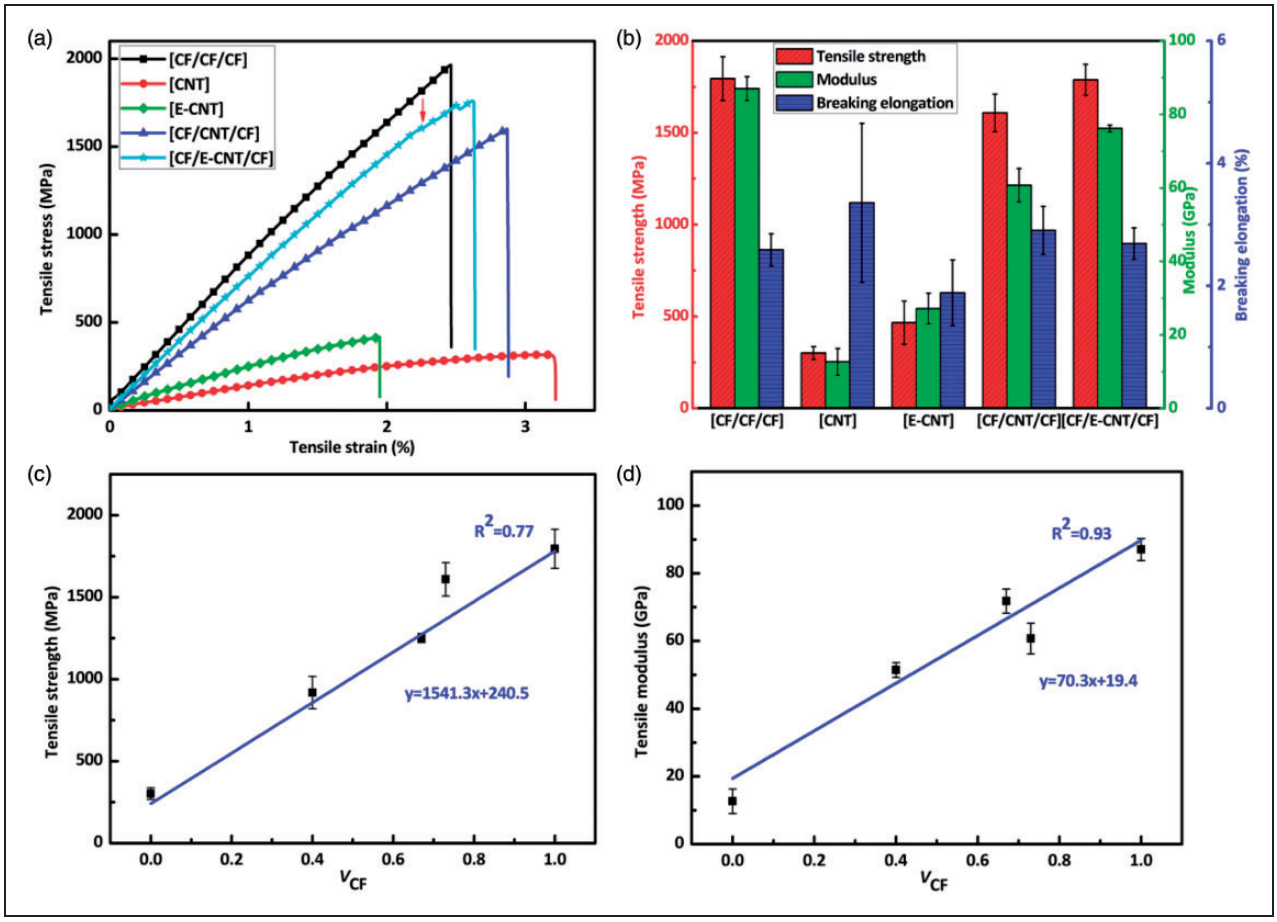

Figure 4. (a) Stress–strain curves and (b) tensile performances of typical CNT film/CF interply hybrid composites and the corresponding control composites. The variation of (c) tensile strength and (d) Young's modulus with the volume fraction of CF ply. CF: carbon fiber; CNT: carbon nanotube.

By following the set process schedule, CF layer had an average thickness of 19.3 μm.

The tensile strength of pristine CNT film/CF interply hybrid composites can be predicted by equation (2) or (3).

$$\sigma_1 = \sigma_{CNT} \bullet (1 - V_{CF}) \qquad (V_{CF} < V_{min}) \tag{2}$$

$$\begin{aligned} \sigma_2 &= \sigma_{CF} \bullet V_{CF} + (\sigma_{CNT})_{\varepsilon^*_{CF}} \bullet (1 - V_{CF}) \\ &= \left(\sigma_{CF} - (\sigma_{CNT})_{\varepsilon^*_{CF}}\right) \bullet V_{CF} + (\sigma_{CNT})_{\varepsilon^*_{CF}} \end{aligned} \qquad (V_{CF} > V_{min}) \tag{3}$$

where σ_1 and σ_2 are tensile strengths when gradual and sudden failure occurred, respectively; V_{min} is the critical thickness ratio of CF ply when $\sigma_1 = \sigma_2$. V_{min} was calculated to be 0.39% for pristine CNT film/CF hybridization; σ_{CNT} and σ_{CF} are the tensile strengths of CNT and CF ply, respectively; $(\sigma_{CNT})_{\varepsilon^*_{CF}}$ corresponds to the tensile stress of CNT ply when CF ply breaks. For [CF/CNT/CF], crack initiated in CF ply due to its relatively low elongation. A relatively high thickness ratio of CF ply may lead to a single crack in CF ply through the whole thickness, resulting in sudden and brittle failure. Thus, the theoretical tensile strength of [CF/CNT/CF] can be written as equation (3).

On the other hand, the tensile strength of epoxidized CNT film/CF interply hybrid composites can be predicted by equation (4) or (5).

$$\sigma_3 = \sigma_{E-CNT} \bullet (1 - V_{CF}) + (\sigma_{CF})_{\varepsilon^*_{E-CNT}} \bullet V_{CF} \quad \left(V_{CF} < V'_{min}\right) \tag{4}$$

$$\sigma_4 = \sigma_{CF} \bullet V_{CF} \qquad \left(V_{CF} > V'_{min}\right) \tag{5}$$

herein, σ_3 and σ_4 are tensile strengths when sudden and gradual failure occurred, respectively; V'_{min} is the critical thickness ratio of CF ply and calculated to be 66.95% for epoxidized CNT film/CF hybridization; σ_{E-CNT} is the tensile strength of E-CNT ply; $(\sigma_{CF})_{\varepsilon^*_{E-CNT}}$ corresponds to the tensile stress of CF ply when E-CNT ply breaks. For [CF/E-CNT/CF],

E-CNT ply had lower elongation than CF ply, and thus crack occurred first in E-CNT layer followed by gradual failure. After the breakage of E-CNT layer, CF layer could go on bearing the load due to high thickness ratio of CF ply. The theoretical tensile strength of [CF/E-CNT/CF] composite can be calculated as equation (5).

As shown in Figure 4(c) and (d), both the tensile strength and Young's modulus showed linear relationships with V_{CF}, as predicted in equations (1) and (3). The linear regression coefficients of strength and modulus were 0.77 and 0.93, respectively, which indicated that tensile properties of hybrid composites with different thickness ratio of CF ply could be well predicted by the proposed simulation.

Table 2 lists the hybrid effect coefficient of [CF/CNT/CF] and [CF/E-CNT/CF] composites. Hybrid effect coefficient of strength (R_s), modulus (R_m), and breaking elongation (R_e) can be calculated as equations (6) to (8).

$$R_s = \frac{\sigma_H - \sigma_T}{\sigma_T} \tag{6}$$

$$R_m = \frac{E_H - E_T}{E_T} \tag{7}$$

$$R_e = \frac{\varepsilon_H - \varepsilon_{LE}}{\varepsilon_{LE}} \tag{8}$$

where subscript "H" and "T" represent experimental and theoretical values, respectively. ε_H is breaking elongation of hybrid composite and ε_{LE} is breaking elongation of low elongation layer.

Table 2. Comparisons of hybrid effect of interply hybrid composites [CF/CNT/CF] and [CF/E-CNT/CF].

Specimens	[CF/CNT/CF]	[CF/E-CNT/CF]
V_{CF}	0.73	0.73
Tensile strength (MPa)	1609	1789
Theoretical strength (MPa)	1391	1302
Hybrid effect coefficient of strength (R_s)	0.16	0.37
Modulus (GPa)	61	76
Theoretical modulus (GPa)	67	71
Hybrid effect coefficient of modulus (R_m)	−0.09	0.08
Breaking elongation (%)	2.9	2.7
Breaking elongation of low elongation layer (%)	2.6	1.9
Hybrid effect coefficient of breaking elongation (R_e)	0.12	0.43

CF: carbon fiber; CNT: carbon nanotube.

Figure 5 illustrates the failure modes of interply hybrid composites. For [CF/CNT/CF], the sudden failure was caused by a single crack in CF ply through the whole specimen thickness (Figure 5(a)). [CF/CNT/CF] showed higher breaking elongation than that of [CF/CF/CF]. This suggested that CNT ply with higher strain may prevent crack propagation by bridging cracks. And thus, both breaking elongation ($R_e = 0.12$) and tensile strength ($R_s = 0.16$) showed positive hybrid effects. On the other hand, due to the weak interfacial bonding, CF and CNT ply were in poor coordination under tensile load, causing the negative hybrid effect of modulus ($R_m = -0.09$). Different from [CF/CNT/CF], [CF/E-CNT/CF] exhibited a gradual failure behavior. After the breakage of E-CNT ply, CF ply carried full external load (Figure 5(b)). The tensile strength of [CF/E-CNT/CF] showed a more significant positive effect ($R_s = 0.37$). Considering the improved interfacial bonding by CNT functionalization, it can be inferred that multiple fractures may occur. The mechanism was illustrated in Figure 5(c) and (d). When crack was first formed in E-CNT ply, it did not propagate into CF layer or cause global delamination. The fracture energy was diverted by the rupture of E-CNT ply, and the load was transferred back into E-CNT ply via the strong interfacial bonding. This contributed to the strong synergistic effect between E-CNT and CF plies. Moreover, modulus of [CF/E-CNT/CF] also showed synergistic effect and exhibited a positive hybrid effect ($R_m = 0.08$). It should be pointed out that failure of [CF/E-CNT/CF] initiated at much higher strain compared to [E-CNT], and finally displayed a positive hybrid effect ($R_e = 0.43$). This should be caused by the protection of thin CF plies, and the formation and propagation of cracks were delayed due to their lower energy release rates. Therefore, we could conclude that the improved tensile performance and synergistic effect of [CF/E-CNT/CF] were attributed to good load transfer and suppressed delamination induced by good interfacial bonding.[32,38,39,48,49]

The improvements of interfacial bonding and load transfer were also evidenced by the fracture surfaces of these hybrid composites, as shown in Figure 6. [CF/CF/CF] showed a typical lateral brittle fracture (Figure 6(a)). [CNT] showed random pullout CNTs with an average length of about 29 μm (Figure 6(b)). For the epoxidized CNT film composite [E-CNT], CNTs were pulled out with a shorter length of about 22 μm, suggesting better load transfer (Figure 6(c)). For the interply hybrid composite [CF/CNT/CF], an overall brittle fracture mode happened, accompanied with delamination (Figure 6(d)), which indicated the slightly uncoordinated deformation between CNT and CF layers induced by weak interfacial bonding. Notably,

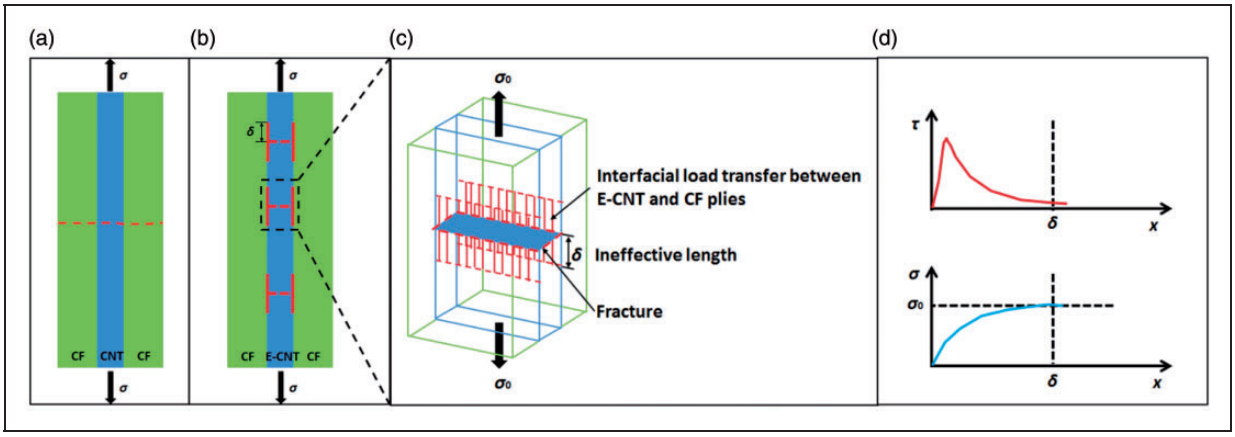

Figure 5. Illustrations on failure modes of interply hybrid composites: (a) sudden failure mode of [CF/CNT/CF] caused by single crack in CF ply and (b) gradual failure mode of [CF/E-CNT/CF] with multiple fractures in E-CNT ply induced by good interfacial bonding, (c) interfacial load transfer between E-CNT and CF plies, and (d) tensile load transferred back into E-CNT layer across the interface by shear stress transfer.
CF: carbon fiber; CNT: carbon nanotube.

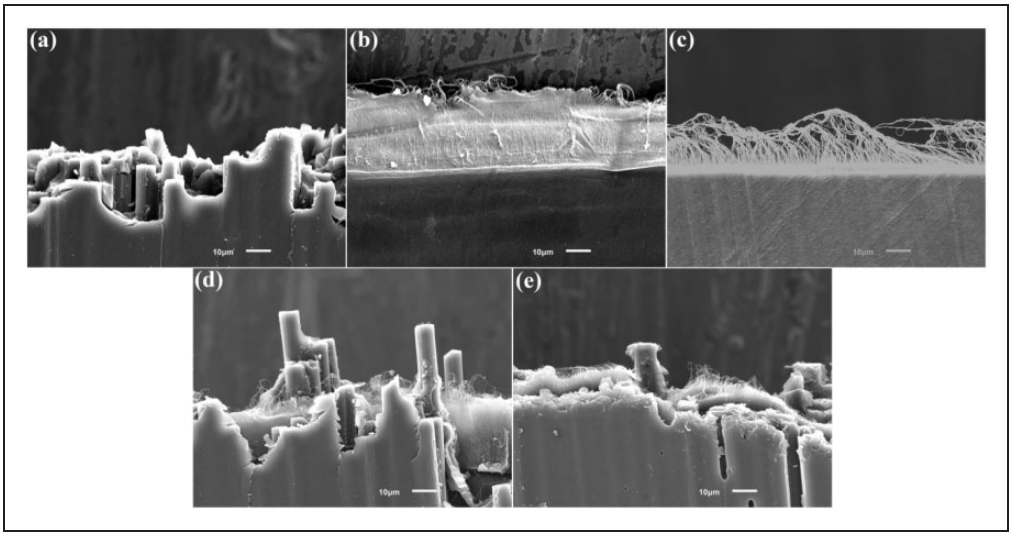

Figure 6. Failure morphologies of composites: (a) [CF/CF/CF], (b) [CNT], (c) [E-CNT], (d) [CF/CNT/CF], and (e) [CF/E-CNT/CF].
CF: carbon fiber; CNT: carbon nanotube.

the hybrid composite [CF/E-CNT/CF] exhibited a more even lateral brittle fracture (Figure 6(e)), demonstrating better interfacial bonding and load transfer caused by the epoxidation of CNT film.

Dynamic mechanical properties of CNT film/CF interply hybrid composites

Figure 7 shows the DMA results of hybrid composites and control samples. Tanδ curve of [CF/CNT/CF] manifested higher damping capacity than [CF/CF/CF]. [CF/CNT/CF] had the maximum tanδ of 0.13, much higher than 0.08 of [CF/CF/CF]. This resulted from the effective integration of CNT film as viscoelastic layer between CF layers. The excellent damping performance of [CF/CNT/CF] was believed to be correlated with the energy dissipation caused by interfacial stick-slip at the nanotube–nanotube interface[4,5,7,50] and the interfacial sliding at the nanotube–polymer interface.[22,41] Such damping is crucial for many commercial applications, such as isolating objects from vibration.[30] For [CF/E-CNT/CF], tanδ curve displayed lower loss factor, which was in good agreement with the result of [E-CNT], indicating the improved interfacial bonding between CNTs and epoxy resin matrix. We demonstrated here interfacial slip, although detrimental to stiffness, may result in very high mechanical damping.[7] Furthermore, the hybrid composite

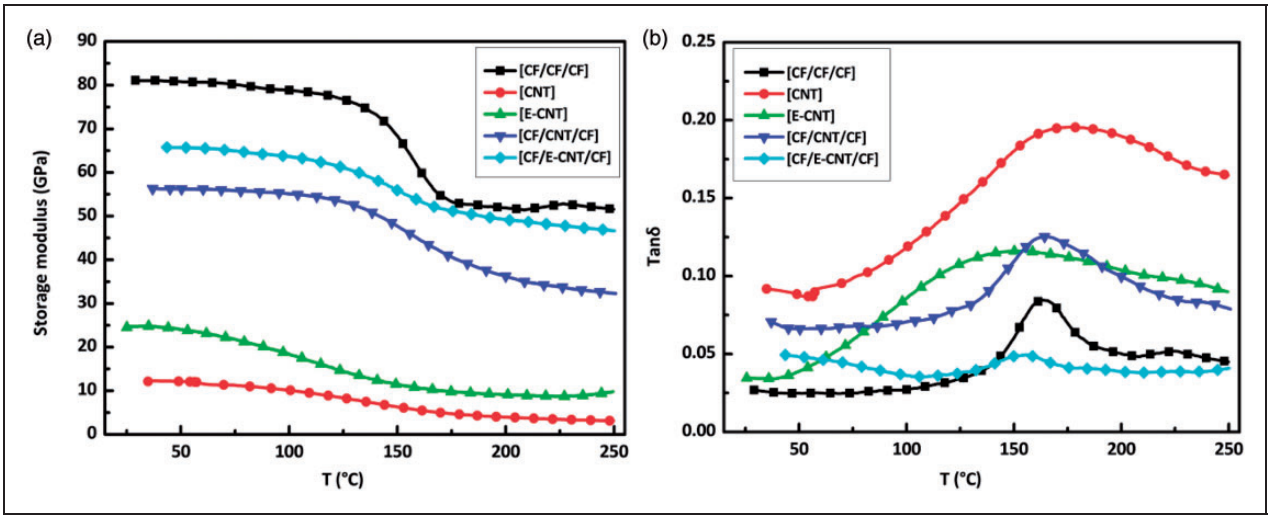

Figure 7. Comparison of (a) storage modulus curves and (b) tanδ curves.

[CF/CNT/CF] exhibited a storage modulus of 56 GPa and a Tg of 164°C. Compared with commercially available viscoelastic damping polymers such as 3 M ISD-112 and 113,[51,52] [CF/CNT/CF] showed higher modulus and temperature limit and provided a promising lightweight structural damping material in electronics, aerospace, and transportation fields.

Electrical conductivity of CNT film/CF interply hybrid composites

Figure 8(a) shows the in-plane electrical conductivities of pristine CNT film/CF hybrid composites with different global CNT contents. As global CNT content increased, all the in-plane electrical conductivities in the direction of 0° ($\sigma_{0°}$), 45° ($\sigma_{45°}$), and 90° ($\sigma_{90°}$) increased. Remarkably, the in-plane electrical conductivities exhibited isotropy with maximum and minimum in the direction of 0° and 90°, respectively. This is because the electrical conductivities of hybrid composite were greatly affected by the anisotropy of CFs and the ply scheme.[53] Compared with [CF/CF/CF] composite, the in-plane electrical conductivities $\sigma_{0°}$, $\sigma_{45°}$, and $\sigma_{90°}$ of hybrid composite with global CNT content of 21 wt% increased to 742, 431, and 277 S cm^{-1}, which were enhanced by 2.6 times, and two and three orders of magnitude, respectively. The electrical conductivities of the CNT film/polyarylacetylene composite,[6] MWCNT sheet/bismaleimide nanocomposite,[31] and CNT film/epoxy composite with 55 wt% resin content[41] were reported to be 700, 915, and 912 S cm^{-1}, respectively. The electrical conductivity of hybrid composites reached the same order of magnitude as CNT film composite.

Figure 8(b) shows the in-plane electrical conductivities of [CF/CF/CF], [CF/CNT/CF], and [CF/E-CNT/CF]. Compared with [CF/CF/CF], the electrical conductivity of [CF/CNT/CF] increased significantly. For interply hybrid composite [CF/CNT/CF], conductive paths were constructed by the highly conductive CNT film and CFs. The bridging between CNTs and CFs could connect CF layer and CNT layer effectively, which can be observed in the cross-sectional morphology, as shown in Figure 8(c).

Figure 8(d) and (e) illustrates the electrical conductivity modes of interply hybrid composite [CF/CNT/CF] in the direction of 0° and 90°. In 0° direction (Figure 8(d)), CFs were oriented parallel to each other, thus CF layer and CNT layer could both form long-distance conducting paths, eventually leading to a higher electrical conductivity. However, in 90° direction (Figure 8(e)), the conduction of CF was limited by large interface resistance. The conducting paths consisted of short-distance fiber paths and long-distance CNT film paths, which were connected by bridging between CNT and CF ply. Based on the above analysis, we could conclude that the electrical conductivity improvement was attributed to suitable CNT loading in CNT ply,[41] dense packing of CFs in CF ply, and bridging effects between CNTs and CFs in hybrid composite.

In addition, the electrical conductivity enhancement of [CF/E-CNT/CF] was less significant than [CF/CNT/CF]. This was caused by its lower local CNT content in CNT ply and functionalization treatment. Still, [CF/E-CNT/CF] had an excellent conductive property with $\sigma_{0°}$, $\sigma_{45°}$, and $\sigma_{90°}$ of 278, 104, and 39 S cm^{-1}, respectively. Similar phenomenon has been reported in a previous study,[43] where CNT/BMI composites showed a reduced electrical conductivity after functionalization.

Therefore, the excellent electrical conductivities and adaptability by layup design endow the hybrid

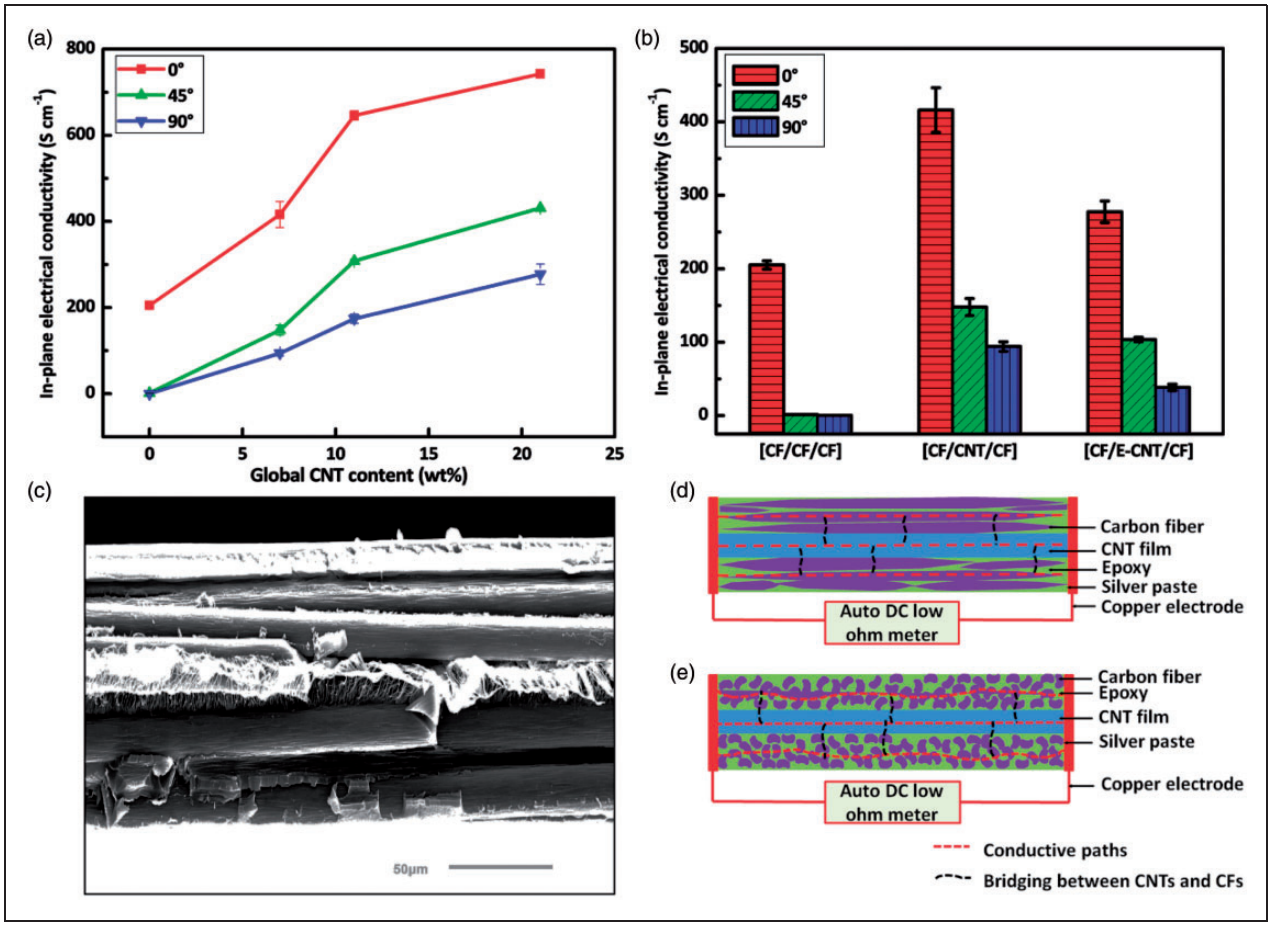

Figure 8. (a) In-plane electrical conductivities of CNT film/CF interply hybrid composites in the direction of 0°, 45°, and 90° as functions of global CNT content; (b) comparisons of the in-plane electrical conductivities of [CF/CF/CF], [CF/CNT/CF], [CF/E-CNT/CF] in the directions of 0°, 45°, and 90°; (c) bridging between CNTs and CFs in [CF/CNT/CF] composite; (d) schematic illustrations on electrical conductivity mode of [CF/CNT/CF] in the direction of 0°; and (e) 90°. Illustrations are not to scale.
CF: carbon fiber; CNT: carbon nanotube.

composite great potential for lightning strike protection, SHM, ESD, EMI shielding, and so on.

Conclusion

In summary, a flexible CNT film and ultrathin CF interply hybrid composite with high CNT content was fabricated. The hybrid composite [CF/CNT/CF] showed average tensile strength of 1609 MPa and modulus of 61 GPa. After epoxidation, the modified hybrid composite [CF/E-CNT/CF] exhibited a higher tensile strength of 1789 MPa and modulus of 76 GPa. The tensile properties of both samples were comparable to the unidirectional T300 CFRPs. It was found that pristine CNT film/CF interply hybrid composite, [CF/CNT/CF], showed sudden and brittle failure, while epoxidation caused a gradual failure behavior of [CF/E-CNT/CF]. Hybrid effect analysis suggested that improved tensile performance and synergistic effect of epoxidized CNT film/CF hybrid composite were attributed to good load transfer and suppressed delamination induced by good interfacial bonding. Furthermore, pristine CNT film/CF hybrid composite [CF/CNT/CF] manifested high damping capacity with the maximum tanδ of 0.13. The in-plane electrical conductivities σ_{0°, σ_{45°, and σ_{90° of hybrid composite with global CNT content of 21 wt% increased to 742, 431, and 277 S cm^{-1}, reaching the same order of magnitude as CNT film composite. Integration of high mechanical properties, good damping performance, and superior electrical conductivity endows the excellent lightweight hybrid composites potentials to be utilized in aerospace, transportation, and electronics industries.

Declaration of conflicting interests

The author(s) declared no potential conflicts of interest with respect to the research, authorship, and/or publication of this article.

Funding

The author(s) disclosed receipt of the following financial support for the research, authorship, and/or publication of this article: The National Natural Science Foundation of China (Grant No. 51103003 and 51403009).

References

1. Bacon R. Growth, structure, and properties of graphite whiskers. *J Appl Phys* 1960; 31: 283–290.
2. Yu MF, Lourie O, Dyer MJ, et al. Strength and breaking mechanism of multiwalled carbon nanotubes under tensile load. *Science* 2000; 287: 637–640.
3. Zhang X, Li Q, Tu Y, et al. Strong carbon-nanotube fibers spun from long carbon-nanotube arrays. *Small* 2007; 3: 244–248.
4. Xu M, Futaba DN, Yamada T, et al. Carbon nanotubes with temperature-invariant viscoelasticity from –196° to 1000°C. *Science* 2010; 330: 1364–1368.
5. Liu Q, Li M, Gu Y, et al. Interlocked CNT networks with high damping and storage modulus. *Carbon* 2015; 86: 46–53.
6. Cai WF, Li M, Wang SK, et al. Strong, flexible and thermal-resistant CNT/polyarylacetylene nanocomposite films. *RSC Adv* 2016; 6: 4077–4084.
7. Suhr J, Koratkar N, Keblinski P, et al. Viscoelasticity in carbon nanotube composites. *Nat Mater* 2005; 4: 134–137.
8. Sun L, Gibson RF, Gordaninejad F, et al. Energy absorption capability of nanocomposites: a review. *Compos Sci Technol* 2009; 69: 2392–2409.
9. De Volder MF, Tawfick SH, Baughman RH, et al. Carbon nanotubes: present and future commercial applications. *Science* 2013; 339: 535–539.
10. Lee JI, Yang SB and Jung HT. Carbon nanotubes-polypropylene nanocomposites for electrostatic discharge applications. *Macromolecules* 2009; 42: 8328–8334.
11. Li N, Huang Y, Du F, et al. Electromagnetic interference (EMI) shielding of single-walled carbon nanotube epoxy composites. *Nano Lett* 2006; 6: 1141–1145.
12. Hou C, Li T, Zhao T, et al. Microwave absorption properties of rare metal-doped multi-walled carbon nanotube/polyvinyl chloride composites. *J Reinf Plast Compos* 2012; 31: 1526–1531.
13. Thostenson ET and Chou TW. Carbon nanotube networks: sensing of distributed strain and damage for life prediction and self healing. *Adv Mater* 2006; 18: 2837–2841.
14. Thostenson ET and Chou TW. Real-time in situ sensing of damage evolution in advanced fiber composites using carbon nanotube networks. *Nanotechnology* 2008; 19: 8099–8104.
15. Wu C, Lu H, Liu Y, et al. Study of carbon nanotubes/short carbon fiber nanocomposites for lightning strike protection. In: *Proc SPIE 7644, behavior and mechanics of multifunctional materials and composites,* California, USA, San Diego, 76441H, March 2010, pp. 1–8. Bellingham WA: SPIE.
16. Njuguna J, Pielichowski K and Alcock JR. Epoxy-based fibre reinforced nanocomposites. *Adv Eng Mater* 2007; 9: 835–847.
17. Chang MS. An investigation on the dynamic behavior and thermal properties of MWCNTs/FRP laminate composites. *J Reinf Plast Compos* 2010; 29: 3593–3599.
18. Bekyarova E, Thostenson ET, Yu A, et al. Multiscale carbon nanotube-carbon fiber reinforcement for advanced epoxy composites. *Langmuir* 2007; 23: 3970–3974.
19. Thostenson ET, Li WZ, Wang DZ, et al. Carbon nanotube/carbon fiber hybrid multiscale composites. *J Appl Phys* 2002; 91: 6034–6037.
20. Garcia EJ, Wardle BL and John Hart A. Joining prepreg composite interfaces with aligned carbon nanotubes. *Compos Pt A Appl Sci Manuf* 2008; 39: 1065–1070.
21. Abot JL, Song Y, Schulz MJ, et al. Novel carbon nanotube array-reinforced laminated composite materials with higher interlaminar elastic properties. *Compos Sci Technol* 2008; 68: 2755–2760.
22. Zeng Y, Ci LJ, Carey BJ, et al. Design and reinforcement: vertically aligned carbon nanotube-based sandwich composites. *ACS Nano* 2010; 4: 6798–6804.
23. An Q, Rider AN and Thostenson ET. Electrophoretic deposition of carbon nanotubes onto carbon-fiber fabric for production of carbon/epoxy composites with improved mechanical properties. *Carbon* 2012; 50: 4130–4143.
24. Lee W, Lee S-B, Choi O, et al. Formicary-like carbon nanotube/copper hybrid nanostructures for carbon fiber-reinforced composites by electrophoretic deposition. *J Mater Sci* 2010; 46: 2359–2364.
25. Boroujeni AY, Tehrani M, Nelson AJ, et al. Hybrid carbon nanotube-carbon fiber composites with improved in-plane mechanical properties. *Compos Pt B Eng* 2014; 66: 475–483.
26. Khan SU, Li CY, Siddiqui NA, et al. Vibration damping characteristics of carbon fiber-reinforced composites containing multi-walled carbon nanotubes. *Compos Sci Technol* 2011; 71: 1486–1494.
27. Song L, Ci L, Lv L, et al. Direct synthesis of a macroscale single-walled carbon nanotube non-woven material. *Adv Mater* 2004; 16: 1529–1534.
28. Nasibulin AG, Kaskela A, Mustonen K, et al. Multifunctional free-standing single-walled carbon nanotube films. *ACS Nano* 2011; 5: 3214–3221.
29. Xu H, Tong X, Zhang Y, et al. Mechanical and electrical properties of laminated composites containing continuous carbon nanotube film interleaves. *Compos Sci Technol* 2016; 127: 113–118.
30. Ajayan PM and Tour JM. Materials science – nanotube composites. *Nature* 2007; 447: 1066–1068.
31. Cheng Q, Bao J, Park J, et al. High mechanical performance composite conductor: multi-walled carbon nanotube sheet/bismaleimide nanocomposites. *Adv Funct Mater* 2009; 19: 3219–3225.
32. Bao JW, Cheng QF, Wang XP, et al. Mechanical properties of functionalized nanotube buckypaper composites. In: *ICCM-17 – 17th International Conference on*

Composite Materials, Edinburgh, UK, 27–31 July 2009, E1: 31. ICCM.
33. Wang S, Downes R, Young C, et al. Carbon fiber/carbon nanotube buckypaper interply hybrid composites: manufacturing process and tensile properties. *Adv Eng Mater* 2015; 17: 1442–1453.
34. Tang P, Zhang R, Shi R, et al. Synergetic effects of carbon nanotubes and carbon fibers on electrical and self-heating properties of high-density polyethylene composites. *J Mater Sci* 2014; 50: 1565–1574.
35. Marom G, Fischer S, Tuler FR, et al. Hybrid effects in composites: conditions for positive or negative effects versus rule-of-mixtures behaviour. *J Mater Sci* 1978; 13: 1419–1426.
36. Wisnom MR, Czel G, Swolfs Y, et al. Hybrid effects in thin ply carbon/glass unidirectional laminates: accurate experimental determination and prediction. *Compos Pt A Appl Sci Manuf* 2016; 88: 131–139.
37. Abdullah-Al-Kafi. Study on the mechanical properties of jute/glass fiber-reinforced unsaturated polyester hybrid composites: effect of surface modification by ultraviolet radiation. *J Reinf Plast Compos* 2006; 25: 575–588.
38. Sihn S, Kim R, Kawabe K, et al. Experimental studies of thin-ply laminated composites. *Compos Sci Technol* 2007; 67: 996–1008.
39. Yokozeki T, Aoki Y and Ogasawara T. Experimental characterization of strength and damage resistance properties of thin-ply carbon fiber/toughened epoxy laminates. *Compos Struct* 2008; 82: 382–389.
40. Liu Q, Li M, Gu Y, et al. Highly aligned dense carbon nanotube sheets induced by multiple stretching and pressing. *Nanoscale* 2014; 6: 4338–4344.
41. Li M, Wang Z, Liu Q, et al. Carbon nanotube film/epoxy composites with high strength and toughness. *Polym Compos*. Epub ahead of print 27 May 2015. DOI: 10.1002/pc.23617..
42. Ogrin D, Chattopadhyay J, Sadana AK, et al. Epoxidation and deoxygenation of single-walled carbon nanotubes: quantification of epoxide defects. *J Am Chem Soc* 2006; 128: 11322–11323.
43. Cheng Q, Wang B, Zhang C, et al. Functionalized carbon-nanotube sheet/bismaleimide nanocomposites: mechanical and electrical performance beyond carbon-fiber composites. *Small* 2010; 6: 763–767.
44. Cheng Q, Li M, Jiang L, et al. Bioinspired layered composites based on flattened double-walled carbon nanotubes. *Adv Mater* 2012; 24: 1838–1843.
45. Gui X, Wei J, Wang K, et al. Carbon nanotube sponges. *Adv Mater* 2010; 22: 617–621.
46. Li H, Gui X, Zhang L, et al. Carbon nanotube sponge filters for trapping nanoparticles and dye molecules from water. *Chem Commun* 2010; 46: 7966–7968.
47. Czél G and Wisnom MR. Demonstration of pseudo-ductility in high performance glass/epoxy composites by hybridisation with thin-ply carbon prepreg. *Compos Pt A Appl Sci Manuf* 2013; 52: 23–30.
48. Manders PW and Bader MG. The strength of hybrid glass/carbon fibre composites. *J Mater Sci* 1981; 16: 2233–2245.
49. Manders PW and Bader MG. The strength of hybrid glass/carbon fibre composites. *J Mater Sci* 1981; 16: 2246–2256.
50. Falvo MR, Taylor RM 2nd, Helser A, et al. Nanometre-scale rolling and sliding of carbon nanotubes. *Nature* 1999; 397: 236–238.
51. Napolitano KL and Kosmatka JB. Co-cured extension-twist coupled damped composite strut. *J Compos Mater* 1998; 32: 1914–1932.
52. Koratkar N, Wei BQ and Ajayan PM. Carbon nanotube films for damping applications. *Adv Mater* 2002; 14: 997–1000.
53. Nascimento JF, Ezquerra TA, Baltà-Calleja FJ, et al. Anisotropy of electrical conductivity and structure in polymer-carbon fiber composite materials. *Polym Compos* 1995; 16: 109–113.